International Journal of Multidisciplinary Research and Growth Evaluation.

Influence of welding speed on corrosion susceptibility of 304l stainless steel in chloride environment

Kutelu BJ [1*], Oke OO [2], Oyetunji A [3]
[1, 2] Department of Mineral and Petroleum Engineering Technology. The Federal Polytechnic, Ado-Ekiti, Ekiti, State, Nigeria
[3] Department of Metallurgical and Materials Engineering. The Federal University of Technology, Akure, Ondo State, Nigeria

* Corresponding Author: **Kutelu BJ**

Article Info

ISSN (online): 2582-7138
Volume: 04
Issue: 05
September-October 2023
Received: 08-09-2023
Accepted: 10-10-2023
Page No: 376-380

Abstract
In this study, corrosion behaviour of 304L austenitic stainless steel, which was obtained from boiler pipe at sugar plant and its weldment samples, which were produced with gas tungsten arc welding (GTAW) technique at varied ranges of GTAW current were investigated in demineralised water - being the operating environment of the boiler. Potentiodynamic polarization measurement was conducted on the samples. And the pitting corrosion attack that was developed on the samples' surfaces at the varied ranges of GTAW current was analysed by Optical microscopy. The results revealed that microstructures of the weldment samples after corrosion at 25^{o}C were characterised by pits of varying sizes and alignment. Inclusions, precipitates and δ ferrite were observed within the microstructures. With increasing and decreasing GTAW speed, values of *Ecorr icorr* and *βa* were shifted to less negative direction (more nobility) and more negative (less nobility) direction respectively. Optimum and least *Ecorr* values of $3.2253x10^{-1}$V Ag/AgCl and $1.7327x10^{-1}$V Ag/AgCl were obtained at GTAW speed of 5.4mm/s and at 1.7 mm/s respectively.

Keywords: austenitic stainless steel, boiler pipe, weldment, demineralised water, potentiodynamic polarization, pitting corrosion, inclusion

1. Introduction

304L austenitic stainless steel (ASS) has been widely used for the construction of welded structures that require to be operated in corrosive environments such as marine (Arpita *et al*., 2016) [4]. Also, it is well suited as material for various manufacturing industries including chemical, petrochemical, medicine and food (Kožuh *et al*., 2013) [16]. In sugar industry for instance, 304L ASS is predominantly used as piping material for transporting steam from the boiler to process house where for the purpose of converting very high pope sugar (VHP) sugar to fortified sugar (FT) (Sami, 2012). Report have shown that surface cracks that were seen on failed portions of a 304L ASS boiler piping (Fig. 1) resulted from pitting corrosion attack (Field report, 2019). Earlier Kožuh *et al*., (2013) [16] and Vladana and Branimir, (2011) have revealed that corrosion susceptibility of the weld joint was due to the resulted microstructure characteristics, hence pits formation could have been accentuated by microstructure transformation during welding. Some of the attendant consequences of failed service piping, particularly at the weld joints are steam leakage, product loss, unscheduled plant shutdown and emergency pipe repairs (Mohd *et al*., 2014) [21].

Traditionally, post-weld heat treatment (PWHT) or local post-weld heat treatment (LPWH) had been employed to obtain the desired microstructure, and hence improve service performance of the weld joints, however, this approach has not yielded the required result, even, as the weld joints still remain potential regions of stress concentration (Astarita *et al*., 2013; Kutelu *et al*., 2018; Balasubramanian *et al*., 2010) [5, 17, 7]. From past research findings, when welding speed is increased at constant arc voltage and current, width of bead and penetration increase until an optimum speed is reached at which penetration will be high, and once optimum speed is attained, further increase in speed will result in decreased penetration (Janunkar *et al*. 2017; Hussain, 2010) [15, 14].

Ahmed *et al*. (2010) [3] have shown that decreasing the welding speed beyond a certain point resulted in decreasing penetration, which was attributed to large amount of weld pool beneath the electrode, which cushions arc penetrating force. And increase in welding speed resulted in decrease in heat input per unit length of the weld, electrode burn off rate and weld reinforcement (Shin *et al*., 2012) [26]. Also, increase in welding speed for the same current and voltage resulted in decrease in heat input, and excessive high welding speed resulted in decreased wetting action, increased tendency of undercut and porosity, and uneven bead shapes (Kutelu *et al*., 2018; Devakumar and Jabaraj, 2014; Bang *et al*., 2008) [17, 10, 8].

Based on findings of the past researchers, it is obvious that proper selection of welding speed is critical for achieving effective weld joint performance. Therefore, in the work, efforts were made to examine effects of varied gas tungsten arc welding (GTAW) speed on pitting corrosion susceptibility of 304L stainless pipe in chloride environment (demineralized water) of the boiler. This is with a view to obtaining optimum speed for application in operating environment of the boiler.

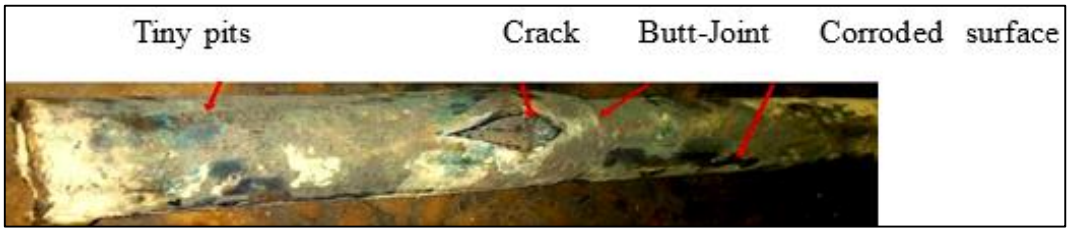

Fig 1: Sample of a failed portion of boiler pipe

2. Experimental Procedure

2.1. Chemical composition of the 304L boiler pipe and filler metal

The chemical composition of the 304L austenitic stainless steel boiler pipe and the 308L stainless steel filler metal, which were used for this research are presented in Tables 1 and 2 respectively. The 304L ASS as-received sample was cut from the boiler pipe shown in Fig.1. This nominally matching filler metal was carefully selected in order to prevent the occurrence of galvanic corrosion that is often associated with wide compositional differences between work piece and filler metal.

Table 1: Chemical composition of the 304L ASS boiler pipe

Element	(Wt. %)	Element	(Wt. %)
C	0.026	Nb	0.009
Si	0.511	Al	0.018
Mn	1.311	Cl	0.002
S	<0.001	Mo	0.069
P	0.013	V	0.083
Cr	18.325	Ti	0.036
Ni	8.469	Fe	75.916
Cu	0.135		

Table 2: Chemical composition of filler metal

Element	(Wt. %)
C	<0.03
Si	0.65
Mn	1.65
S	0.03
P	0.03
Cr	19.5-22.0
Ni	9.0-11.0

2.2. Welding

The base plates were cut into sizes of 120 mm × 20 mm × 8 mm and clean with acetone to remove lubricant and surface contamination. Welding was performed using Clark TIG welding machine. Before welding, the base plate were machined to prepare butt joint edges chamfered at 60° and tacked at both ends of the pipe to make a single-V groove of 60°. To obtain good root penetration, the root gap was kept at 2.5 mm (Amer *et al*., 2015) [2]. Welding was carried out using a 2.5 mm diameter filler electrode at constant current and voltage of 160 A and 30 V respectively. During and after the welding, joints were visually inspected for any geometrical non-conformity and weld defects.

2.3. Metallography

The metallographic samples were prepared in accordance with ASTM E3-11 (2011). They were grind on silicon carbide paper of different mesh sizes from 120, 240, 320, 400, 600, 800 to 1200 mesh, and finally polished on emery cloth using a suspension of alumina powder to obtain a mirror-like surface. The samples were etched in solution of 50 ml HCl + 50 ml HNO3 + 50 ml water for two minutes. The microstructures were viewed and captured by optical metallurgical microscope (OMM) (Olympus GX51) with camera attached.

2.4. Potentiodynamic studies

Samples of the pipe weldments were cut with simple handsaw to square samples with dimensions of (10x10x4.5) mm3. They were mounted in resin and connected with a flexible wire. The mounted samples were then ground, polished, cleaned and rinsed properly. A three-electrode cell was used for the studies with the 304L ASS boiler pipe as working electrode, silver/ silver chloride (Ag/AgCl) as reference electrode and as platinum plate counter electrode.

The electrodes were immersed in the chloride-rich demineralised water whose chemical composition is depicted in Table 3 at room temperature (25oC). And before each experiment the working electrodes were polished with emery paper to a 1000 metallographic finish, degreased in ethanol and rinsed with distilled water. Data were recorded using a computer-based data logging system (Autolab PGSTAT 204N) employing NOVA software for corrosion analysis.

Table 3: Average Daily Demineralised Water Routine Analysis Report (30 days)

S/No	Description	Water Parameters						
		pH	TH	TDS	OH	Cl	SO_3	CO_3
1.	Raw water	5.40	6	25.0	0	12		
2.	Treated water	7.02	8	87.0	0	20		
3.	Softened water	9.41	0	0	0	4		
4.	Condensate	6.96	0	0	0	4		
5.	Make-up water	7.00	0	0	0	4		
6.	Boiler feed	10.92	0	20.0	0	6		
7.	Boiler No. 1	11.72	0	589	208	12	8	
8.	Boiler No. 6	11.67	-	593				18
9.	Boiler No. 3	11.55	0	433	88	8	14	16
10.	Boiler No. 4	11.04	0	119	40	5	5	8
11	Boiler No. 5	12.09	0	842	272	46	45	20

3. Results and Discussion

3.1. Post corrosion microstructure characteristics of the weldment

The post corrosion weldment samples, comprising FZ and HAZ at welding speeds of 1.7 mm/s, 3.2 mm/s, mm/s 5.4 mm/sand 7.2 mm/s (Plates 2 AC1-AC5) are characterised by varied volume fraction of austenite and ferrite phases. In addition, pits, inclusions, precipitates and δ-ferrite of varying sizes and alignment are present within the phases. The increased number and size of pits shown by the weldments produced at GTAW speed in the range (1.7-4.6 mm/s) given by Plate 2-4 relative to weldments produced at GTAW speed range (5.4-7.2 mm/s) shown by Plates 5-7 was accounted for by microstructure inhomogeneity (Kožuh *et al*., 2013; Lu *et al*., 2005,) [16]. And The more volume fraction of ferrite phase in the range of 1.7-4.6 mm/s relative to the range of 5.4-7.2 mm/s was attribute to from high heat input with concomitant slow cooling, during which there was more time for austenite to transformation to ferrite during solidification (Tabish *et al*., 2014; Subodh and Shahi, 2011) [28, 27].

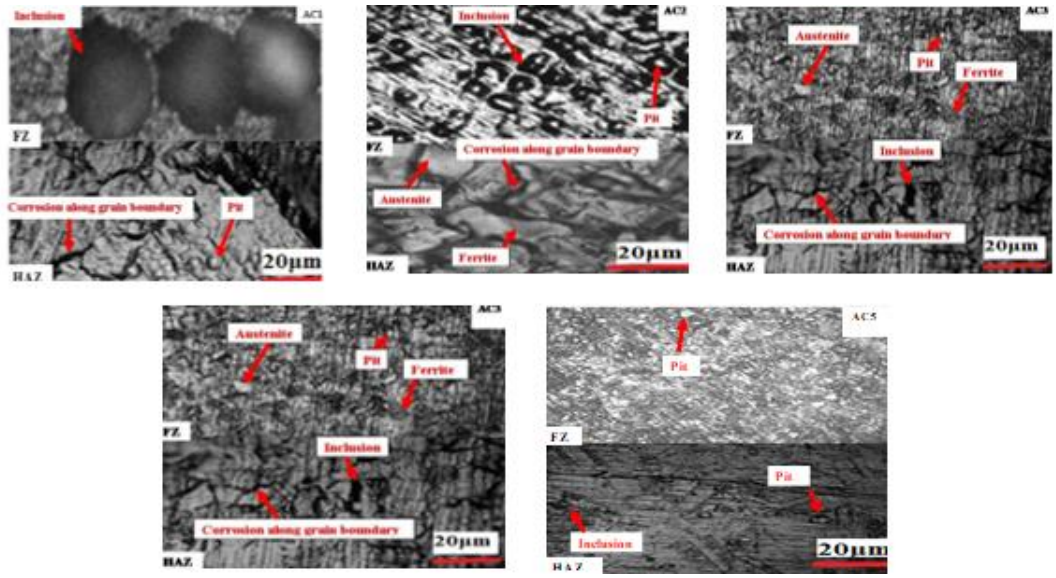

Fig 2: Microstructures of the weldments Produced at GTAW speed of (a) 1.7 mm/s, (b) 3.2 mm/s (c) 4.6 mm/s (d)5.4 mm/s and (e) 7.2 mm/s respectively.

3.2. Electrochemical process of the weldments

The potentiodynamic polarisation curves and corrosion rate of the weldment at varied GTAW speed are depicted in Figs. 3 and 4 respectively. Optimum Ecorr. values of 3.2253x10-1V Ag/AgCl, was obtained at GTAW speed of 5.4mm/s and least of 1.7327x10-1V Ag/AgCl at 1.7 mm/s. Ecorr, icorr and βa values shifted to less negative directions (more nobility) and a more negative direction (less nobility) with increasing and decreasing GTAW speed respectively (Huabing *et al*., 2015). And it is obvious from the characteristic features of the polarisation curves, the weldment is a passive alloy (Fotana, 2005) [13]. Chromium contribution to elemental composition of the experimental sample boiler pipe is 18.325wt. % (refer to Table 1). Chromium reacted with dissolved oxygen in the operating environment of the plant (demineralised water), forming thin oxide film (1-3nm thick), which acted as a barrier between the weldment and demineralised water (Shin *et al*., 2012; Marcus *et al*., 2008; Sato, 2001) [26, 25]. The electrochemical process is described by Eq. 1.

$$3FeO + 2Cr \rightarrow Cr_2O_3 + 3Fe$$

The shift in corrosion potentials (Ecorr.) toward less negative direction (more nobility) at the GTAW speed ranges (5.4-7.2 mm/s) was due to fast cooling conditions with attendant high dislocation density, during which more diffusion paths were provided for migration of chromium to the surface, where double layer corrosion products of Fe2O3 and Cr2O3 were formed (Atapour *et al*., 2015) [6]. And owing to the resulting relative fine-grained microstructures, the formed surface oxides assumed a compact, impervious and homogeneous

features, which accounted for the observed high electrochemcal stability. And the slow cooling conditions with attendant coarse-grained microstructures at GTAW speed range of 1.7-4.6 mm/s accounted for shift in corrosion potential (Ecorr.) toward more negative direction (less nobility). The formed surface oxides assumed loose, pervious and inhomogeneous features, leading to low electrochemcal stability (Saifu *et al*., 2017; Olsson and Landolt, 2003) [23, 22]. In addition, high pitting exhibited by the weldments with coarse-grained microstructures at GTAW speed of range 1.7-4.6 mm/s can be attributed to increased presence of surface oxide breakdown and cracks that resulted from low electrochemcal stability of the formed surface oxides (Liou *et al*., 2001; Sato, 2001) [18, 25]. Also, the more visible inclusions within the microstructures, particularly at GTAW speed of 1.7 mm/s (Plate 1) could have led to weak spots in the passive film and, in consequence, less nobility, as direct exposure of the boundary between the inclusion and matrix to the aggressive DW was palpable (Costa, 2018) [9].

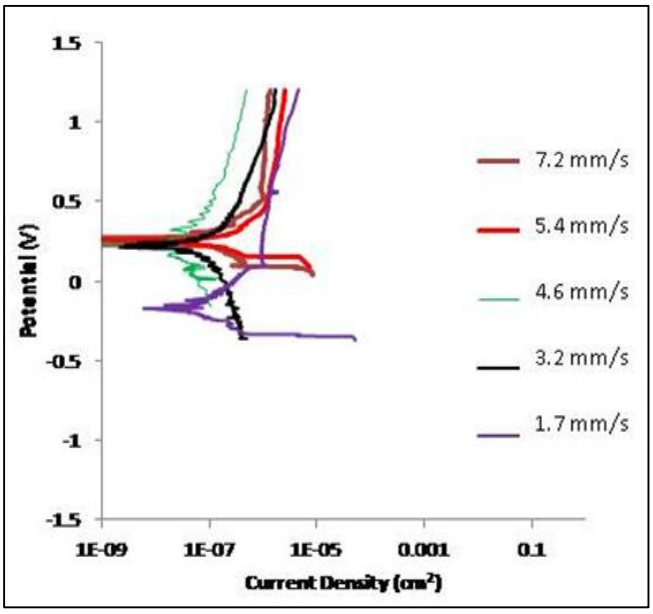

Fig 3: Potentiodynamic polarisation curves of the weldment at varied GTAW speed in demineralised water at 25ºC

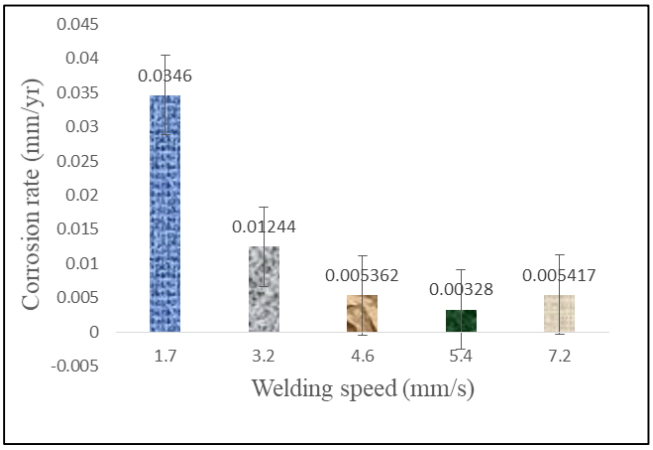

Fig 4: Influence of GTAW speed on corrosion rate of the weldment at 25ºC

4. Conclusions

From the results of the research, the following conclusion were drawn:

1. Microstructures of the weldment samples at the varied GTAW speed after corrosion at 25ºC are characterised by pits of varying sizes with different alignment. Also, inclusions, precipitates and δ ferrite were observed within the microstructures.
2. Generally, values of *Ecorr icorr* and *βa* shifted to less negative directions (more nobility) with increasing GTAW speed and shifted to a more negative direction (less nobility) with decreasing GTAW speed.
3. Pitting susceptibility of the weldment was lowest at the ranges of GTAW speed (5.4 mm/s-7.2 mm/s and highest at the ranges of GTAW speed (1.7 mm/s -4.6 mm/s).
4. Optimum *Ecorr* values of $3.2253x10^{-1}$V Ag/AgCl, was obtained at GTAW speed of 5.4mm/s and least of $1.7327x10^{-1}$V Ag/AgCl at 1.7 mm/s.

References

1. Aamir S, Abdul Aziz MI, Osama Junaid M, Sagheer A. Effect of TIG welding parameters on the properties of 304L automated girth welded pipes using orbital welding. Journal of Material Science. 2017;5(4):136-143.
2. Amer SM, Morsy MA, Hussein MA, Atlam A, Mosa ES. Effect of welding parameters variation on the weldability of austenitic stainless steel 304L. International Journal of Scientific and Engineering Research. 2015;6(2):589-595.
3. Ahmed KH, Abdul L, Mohd J, Pramesh T. Influence of welding speed on tensile strength of welded joint in TIG welding process. International Journal of Applied Engineering Research. 2010;1(3):518-527.
4. Arpita NB, Vikram AP. Influence of process parameters of TIG welding process on mechanical properties of 304LSS welded joint. International Research Journal of Engineering and Technology. c2016;3:977.
5. Astarita A, Squillace A, Montuori M, Bitondo C, Monetta T, Bellucci F. Post welding heat treatment influence on corrosion behaviour of AA 2024 FSW butt joints. Antonello.astarita@unina.it; c2013.
6. Atapour M, Dana MM, Ashrafizadeh F. A corrosion study of grain-refined 304L stainless steels produced by the martensitic process. International Journal of ISSI. 2015;12(2):30-38.
7. Balasubramanian M, Jayabalan V, Balasubramanian V. Effect of process parameters of pulsed current tungsten inert gas welding on weld pool geometry of titanium welds. Acta Metallurgica Sinica (English Letters). 2010;23(4):312.
8. Bang KS, Jung DH, Park C, Chang WS. Effects of welding parameters on tensile strength of weld metal in flux cored welding. Science and Technology of Welding and Joining. 2008;13(6):508-514.
9. Costa S. Non-metallic inclusions in steels-origin and control (review). Journal of Materials Research and Technology. 2018;7:283-299.
10. Devakumar D, Jabaraj DB. Research on gas tungsten arc welding of stainless steel - an overview. International Journal of Scientific and Engineering Research. 2014;5(1):1612-1618.
11. Ebrahimi N, Momeni M, Kosari A, Zakeri M, Moayed MH. A comparative study of critical pitting temperature (CPT) of stainless steels by electrochemical impedance spectroscopy (EIS), potentiodynamic and potentiostatic techniques. Corrosion Science. 2012;59:96-102.

12. Fontana MG. Corrosion Engineering. 3rd ed. Tata McGraw-Hill Publishing Co. Ltd., New Delhi, India; c2005.
13. Huabing Li, Zhouhua J, Hao F, Shucai Z, Peide H, Wei Z, et al. Effect of temperature on the corrosion behaviour of super austenitic stainless steel S32654 in polluted phosphoric acid. International Journal of Electrochemical Science. 2015;10:4832-4848. Available from: www.electrochemsci.org
14. Hussain AK. Influence of welding speed on tensile strength of welded joint in TIG welding process. International Journal of Applied Engineering Research. 2010;1(3):518.
15. Janunkar RG, Allurkar S, Mahesh P. An influence on effect of welding speed on strength of welded joint using TIG welding process. World Journal of Technology, Engineering and Research. 2017;2(1):337-342.
16. Kožuh SM, Gojić M, Vrsalović L, Ivković B. Corrosion failure and microstructure analysis of AISI 316L stainless steels for ship pipeline before and after welding. Kovove Materiály. 2013;51:53-61.
17. Kutelu BJ, Seidu SO, Eghabor GI, Ibitoye AI. Review of GTAW welding parameters. Journal of Minerals and Materials Characterization and Engineering. 2018;6(5):541-554.
18. Liou H, Pan Y, Hsieh R, Tsai W. Effects of alloying elements on the mechanical properties and corrosion behaviours of 2205 duplex stainless steels. Journal of Materials Engineering and Performance. 2001;10:315-322.
19. Lu BT, Chen ZK, Luo JL, Patchett BM, Xu ZH. Pitting and stress corrosion cracking behavior in welded austenitic stainless steel. Journal of Electrochemical Acta. 2005;32(2):210-215.
20. Marcus P, Maurice V, Strehblow HH. Localised corrosion (pitting): A model of passivity breakdown including the role of the oxide layer nanostructure. Corrosion Science. 2008;50(9):2704-2724.
21. Mohd S, Mohd F, Hasan PKB. Effect of welding speed, current and voltage on mechanical properties of underwater welded mild steel specimen (C, Mn, Si) with insulated electrode E6013. MIT International Journal of Mechanical Engineering. 2014;4(2):120-124.
22. Olsson COA, Landolt D. Passive films on stainless steels-chemistry, structure and growth. Electrochimica Acta. 2003;48(9):1093-1104.
23. Saifu D, Shuangbao W, Linyue W, Jianting L, Yujie W. Influence of chloride on passive film chemistry of 304 stainless steel in sulfuric acid solution by glow discharge optical emission spectrometry analysis. International Journal of Electrochemical Science. 2017;12:1106-1117. Available from: www.electrochemsci.org
24. Sami IJ. Failure characteristics of boiler pipes in Al-Emsaeb electric power plants. Journal of Babylon University Engineering Sciences. 2012;20(1):87-99.
25. Sato N. The stability and breakdown of passive oxide films on metals. Journal of the Indian Chemical Society. 2001;78:19-26.
26. Shin YT, Shin HS, Lee HW. Effects of heat input on pitting corrosion in super duplex stainless steel weld metals. Metals and Materials International. 2012;18:1037-1040.
27. Subodh K, Shahi AS. Effect of heat input on the microstructure and mechanical properties of gas tungsten arc welded AISI 304 stainless steel joints. Materials and Design. 2011;32:3617-3623.
28. Tabish TA, Abbas T, Farhan M, Atiq S, Butt TZ. Effect of heat input on microstructure and mechanical properties of the TIG welded joints of AISI 304 stainless steel. International Journal of Scientific and Engineering Research. 2014;5:2014-1532.
29. Vladana NR, Branimir NG. Corrosion of an austenite and ferrite stainless steel weld. Journal of the Serbian Chemical Society. 2011;76(7):1027-1035.